

## DESIGN AND OPTIMIZATION OF HIGHLY SENSITIVE PHOTONIC CRYSTAL FIBER WITH LOW CONFINEMENT LOSS FOR ETHANOL DETECTION

Md. Faizul Huq Arif<sup>1\*</sup>, Sayed Asaduzzaman<sup>1</sup>, Md. Jaminul Haque Biddut<sup>1</sup>, Kawsar Ahmed<sup>1</sup>

<sup>1</sup>*Department of Information and Communication Technology (ICT), Mawlana Bhashani Science and Technology University, Santosh, Tangail-1902, Bangladesh*

(Received: March 2016 / Revised: June 2016 / Accepted: October 2016)

### ABSTRACT

In this paper, two highly sensitive photonic crystal fiber (PCF) structures with microstructure core and cladding have been demonstrated for Ethanol sensing. The microstructure core of both proposed PCFs is designed with supplementary holes in an octagonal formation. We have investigated the relative sensitivity and the confinement loss of the proposed PCF structures employing a full vectorial finite element method (FEM). The proposed PCFs work at a wide transmission band covering 0.8  $\mu\text{m}$  to 2  $\mu\text{m}$  and exhibit high sensitivity and low confinement loss simultaneously. The numerical analysis shows that the circular shape of air holes in the first ring is a more salient attribute for increasing sensitivity and the presence of the square shape of air holes in the first ring shows better performance to reduce confinement loss.

*Keywords:* Confinement loss; Ethanol sensor; Finite Element Method (FEM); Photonic Crystal Fiber (PCF); Sensitivity

### 1. INTRODUCTION

Fiber optic technology revolutionized the fields of telecommunication applications. The invention of photonic crystal fiber (PCF) in 1996 was a breakthrough in fiber optic technology. Photonic crystal fiber (PCF) is the proposition of next generation optical fiber. PCFs can be used as a transmission medium and as optical functional devices (Knight et al., 1996; Birks et al., 1997), a condition which reveals great potentiality in both telecom and non-telecom applications. Due to the enhanced design freedom and unique structural features, PCFs have become extremely popular. In recent years, much research has been conducted for the enhancement of PCF performance. PCF establishes intelligent systems by sensing temperature, motion, electric and magnetic field, pressure, torsion, refractive index, traversal loading, DNA, humidity, various types of gasses and liquids and so on (Pinto & Lopez-Amo, 2012).

A PCF sensor is a smart application of fiber optic technology for sensing and detecting different gasses or liquids. The field of PCF-based sensors is rising in toxic chemical sensing (Balaji et al., 2006; Kong et al., 2000), bio sensing (Hu et al., 2012), structural health monitoring (SHM) (McCague et al., 2014) etc. due to their high sensitivity, flexibility, reduced size, low cost and robustness (Cárdenas-Sevilla et al., 2011). One of the most important safety issues of the chemical industry and gas production is to detect flammable or toxic gas/chemical leakage. In recent years, researchers are intensifying their research, in keeping with much interest on the development of PCF-based sensors for environmental and safety monitoring issues (Whitenett et al., 2003; Carvalho et al., 2009). Index-guided PCFs have the ability to detect gasses or

---

\*Corresponding author's email: arifict27@gmail.com, Tel. +8801823462325  
Permalink/DOI: <https://doi.org/10.14716/ijtech.v7i6.3439>

chemicals in a wide range of wavelengths (Olyae et al., 2014). So it has become a great challenge to the fiber optic researchers to enhance the sensing performance of PCFs.

A large number of studies have been reported to enhance the sensing performance of PCF-based gas and liquid sensors. Morshed et al. (2015a) presented an article on a hollow core-based PCF structure for gas sensing which enhanced relative sensitivity with low confinement loss using a novel combination (hexagonal-octagonal-decagonal) of a cladding structure. In recent years, the concept of filling liquids or gasses in the core or cladding region has attracted much attention to the researchers for chemical sensing applications. The research article (Cordeiro et al., 2006a) proposed a PCF in which both core and cladding were a microstructure and it enhanced the evanescent field, infiltrating it with a liquid sample. This concept offers a great potentiality to broaden the field of liquid sensing applications. Another research article by Ademgil (2014) shows the enhancement of relative sensitivity for liquid sensing, using a microstructure-infiltrated core with octagonal cladding. Recently, Asaduzzaman et al. (2015) proposed a microstructure core PCF with elliptical supplementary holes and found a better sensitivity than the previously one researched by Ademgil (2014) for liquid sensing.

In this research, we have enhanced the relative sensitivity for Ethanol sensing by our proposed two PCFs demonstration. We have considered Ethanol for the targeted chemical species because Ethanol is considered to be one of the major chemical solutions in the chemical industries. Ethanol sensors play an important role in keeping safe the industrial workers from some possible damages, such as headaches, dizziness, confusion, balance disorder and nausea caused by Ethanol vapor (James et al., 2005). We also discussed the impact of sensitivity and confinement loss for circular- and square-shaped air holes in the first ring. It has been investigated numerically and proven that this formation of the microstructured core and cladding exhibits a higher sensitivity.

## 2. DESIGN PRINCIPLE

The proposed two PCFs have the same design criteria, except the first rings air holes. Both of the PCFs contain three rings of air holes in the cladding. The innermost ring is hexagonal in shape and the rest of the two rings are octagonal in shape. Only one geometrical difference occurs between PCF<sub>1</sub> and PCF<sub>2</sub>, which is that the innermost ring of PCF<sub>1</sub> contains circular air holes, whereas PCF<sub>2</sub> has square holes. Figure 1 shows the transverse cross-sectional view of the proposed PCF<sub>1</sub> and PCF<sub>2</sub>, respectively. The diameter of the innermost ring air holes of PCF<sub>1</sub> has been denoted by  $d$  and the length of an edge of square holes in the innermost ring of PCF<sub>2</sub> is  $l$ ; where  $\pi(d/2)^2 = l^2$ .

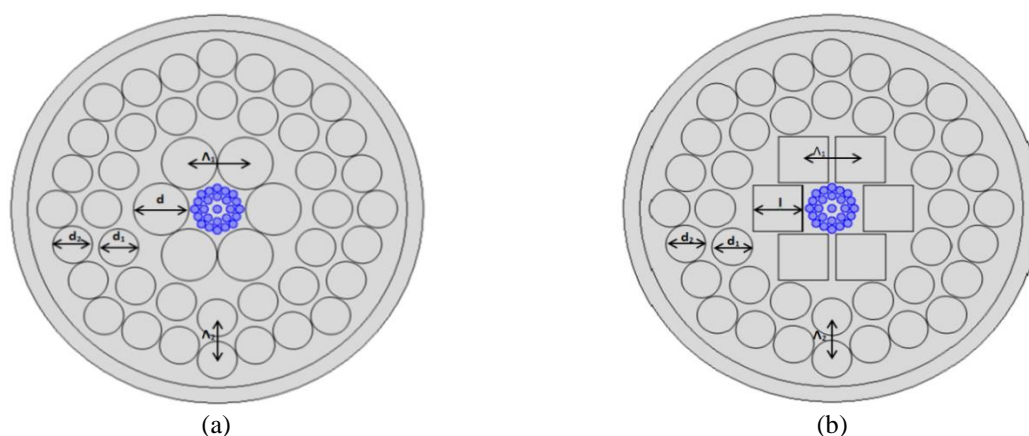


Figure 1 Transverse cross-sectional view of (a) PCF<sub>1</sub> and (b) PCF<sub>2</sub>

The diameters of the air holes of the second and third ring for both of the PCFs are  $d_1$  and  $d_2$  respectively. The pitch between the two adjacent air holes at the first ring is  $\Lambda_1$  and the pitch between two adjacent air holes for both of the two outer octagonal rings is  $\Lambda_2$ ; where,  $\Lambda_1=1.34\Lambda_2$ . The enlarged view of the core region has been shown in Figure 2. The diameter of all the supplementary holes is the same and it has been denoted as  $d_c$ .

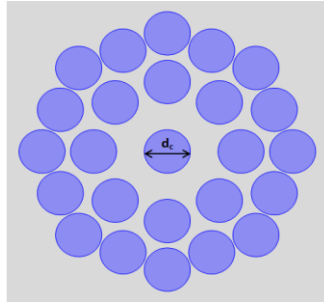


Figure 2 Enlarged view of the core region

### 3. SIMULATION

Our proposed PCFs have been analyzed for Ethanol sensing. A full vectorial finite element method (FEM) has been applied to the circular perfectly matched layer (PML) of the PCFs using an FEM-based simulation software COMSOL *Multiphysics 4.2*. The simulated mode profiles of the proposed PCFs have been shown in Figure 3.

The propagation characteristics of the leaky mode were evaluated by using the PML as boundary condition at a wide range of wavelengths from 0.8  $\mu\text{m}$  to 2  $\mu\text{m}$ . The background material of the proposed PCFs is made of silica. The Sellmeier equation is used to model the background material, as shown in Equation 1 (Sellmeier, 1871).

$$n(\lambda) = \sqrt{1 + \frac{B_1\lambda^2}{\lambda^2 - C_1} + \frac{B_2\lambda^2}{\lambda^2 - C_2} + \frac{B_3\lambda^2}{\lambda^2 - C_3}} \quad (1)$$

where  $n$  is the refractive index,  $\lambda$  ( $\mu\text{m}$ ) is the wavelength,  $B_{(i=1,2,3)}$  and  $C_{(i=1,2,3)}$  are the Sellmeier coefficients. The refractive index of the background material (Silica) and infiltrated Ethanol in the core for different wavelengths have been listed in Table 1.

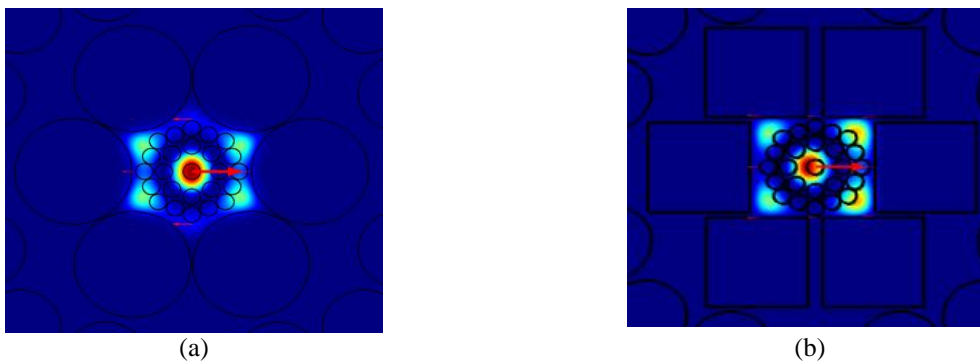


Figure 3 X-polarized modes for (a) PCF<sub>1</sub> and (b) PCF<sub>2</sub>

Modal analysis of the fundamental mode has been performed on the cross section in the  $x$ - $y$  plane of the PCF, as the wave propagates in the  $z$ -direction. We considered here the effective indices of the PCF<sub>1</sub> and PCF<sub>2</sub> for the X-polarization mode and at the wavelength

$\lambda=1.3 \mu\text{m}$ . It was found that the effective refractive indices for PCF<sub>1</sub> and PCF<sub>2</sub> were 1.2951 and 1.3175, respectively.

Table 1 Wavelength vs. refractive index for background silica and infiltrated ethanol

Wavelength ( $\mu\text{m}$ )	Refractive Index (Silica)	Refractive Index (Ethanol)
0.8	1.453	1.357
0.9	1.452	1.356
1.0	1.450	1.355
1.1	1.449	1.354
1.2	1.448	1.353
1.3	1.447	1.353
1.4	1.446	1.352
1.5	1.445	1.352
1.6	1.443	1.351
1.7	1.442	1.350
1.8	1.441	1.349
1.9	1.440	1.348
2.0	1.449	1.347

#### 4. ANALYSIS METHOD

We applied the full vectorial finite element method for its proven reliability (Lee et al., 2009) to analyze the optical properties of the proposed PCFs. Assuming PML as the boundary condition, the complex effective indices ( $n_{eff}$ ) has been obtained from the eigenvalue equation for the magnetic field  $\vec{H}$ , as shown in Equations 2 and 3.

$$\vec{H}(x, y, z, t) = \vec{H}(x, y) \exp[i(\omega t - \beta z)] \tag{2}$$

$$\nabla \times (n^{-2}(\omega) \nabla \times \vec{H}) - K_0^2 \vec{H} = 0 \tag{3}$$

where  $k_0=2\pi/\lambda$  represents the wave number in free space,  $\omega$  is the angular frequency and  $\beta$  is the propagating constant, as shown in Equation 4:

$$\beta = n_{eff} k_0 \tag{4}$$

The leakage of light from the core to exterior materials results in confinement loss (dB/m) which can be obtained from the imaginary part of  $n_{eff}$  using the following Equation 5:

$$L_c = \frac{40\pi}{\ln(10)\lambda} \text{Im}(n_{eff}) \times 10^6 \approx 8.686K_0 \text{Im}(n_{eff}) \times 10^6 \tag{5}$$

The relative sensitivity coefficient measures the interaction between light and the material to be sensed and it can be calculated through the following Equation 6:

$$r = \frac{n_r}{n_{eff}} f \tag{6}$$

where,  $n_r$  represents the refractive index of the material to be detected (Ethanol) within the air holes and  $n_{eff}$  is the modal effective index. The symbol  $f$  is the percentage ratio of the air holes power and the total power, as shown in Equation 7, (Stewart et al., 1991).

$$f = \frac{f_{sample} \operatorname{Re}(E_x H_y - E_y H_x) dx dy}{f_{total} \operatorname{Re}(E_x H_y - E_y H_x) dx dy} \times 100 \quad (7)$$

where  $E_x$ ,  $E_y$  and  $H_x$ ,  $H_y$  are the transverse electric field and magnetic field respectively. Using the finite element method (FEM), the mode field patterns  $E_x$ ,  $E_y$ ,  $H_x$ ,  $H_y$  and effective indices  $n_{eff}$  are obtained.

## 5. RESULTS AND DISCUSSION

The supplementary tiny holes have been filled with Ethanol. Among the guiding properties of PCF, two of them have been investigated in our proposed PCFs which are relative sensitivity and confinement loss.

Figure 4 illustrates the curves of the real part of the effective refractive index of PCF<sub>1</sub> and PCF<sub>2</sub>. It is clear from Figure 4 that the effective refractive index decreases linearly with an increase in wavelength. Moreover, PCF<sub>2</sub> shows higher effective refractive index than PCF<sub>1</sub>.

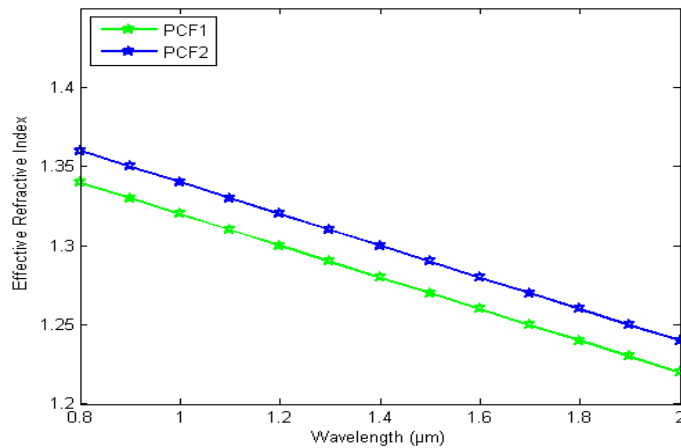


Figure 4 The effective index curves of PCF<sub>1</sub> and PCF<sub>2</sub> for X-polarization mode

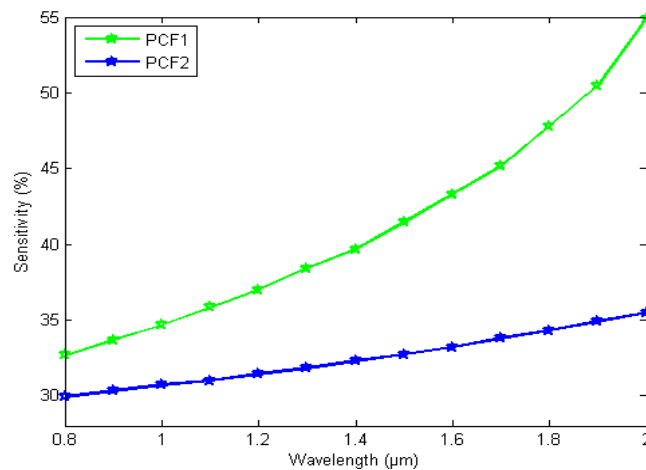


Figure 5 Comparison of the relative sensitivity of PCF<sub>1</sub> and PCF<sub>2</sub> as a function of operating wavelengths for Ethanol sensing

Figure 5 presents the variation of relative sensitivity curves of PCF<sub>1</sub> and PCF<sub>2</sub> as a function of operating wavelength. The relative sensitivity for both of the proposed PCFs increases

incrementally, according to the wavelength. It can be evidently seen that PCF<sub>1</sub> shows a higher relative sensitivity than the PCF<sub>2</sub>. The reason behind that finding is a fraction of evanescent field penetrates to the circular holes, which increases and the relative sensitivity of the PCFs increase consequently.

Figure 6 presents the confinement loss curves as a function of the operating wavelength of the proposed PCF<sub>1</sub> and PCF<sub>2</sub>. However, by investigating Figure 6, it is clear that the PCF<sub>2</sub> exhibits better performance than PCF<sub>1</sub> in terms of confinement loss.

Figure 7 shows the relative sensitivity performance of the proposed PCFs in varying the diameter ( $d_c$ ) of the supplementary holes in the core region at the wavelength  $\lambda = 1.3 \mu\text{m}$ . This investigation describes that the relative sensitivity increases with the increment of the diameter of the supplementary holes.

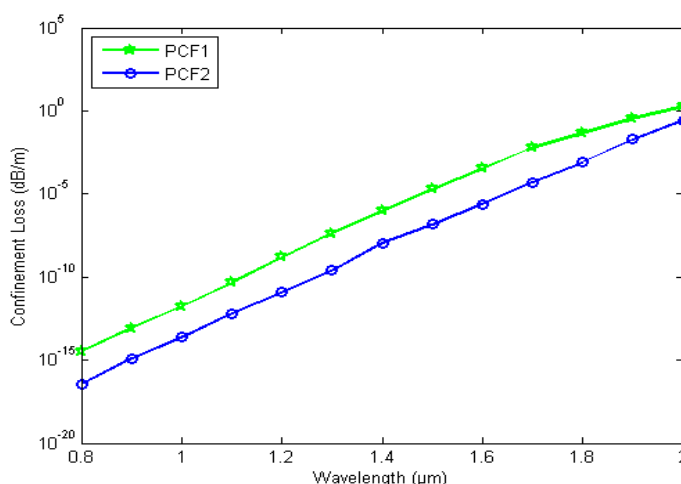


Figure 6 Comparison of confinement loss of PCF<sub>1</sub> and PCF<sub>2</sub> as a function of operating wavelengths for Ethanol sensing

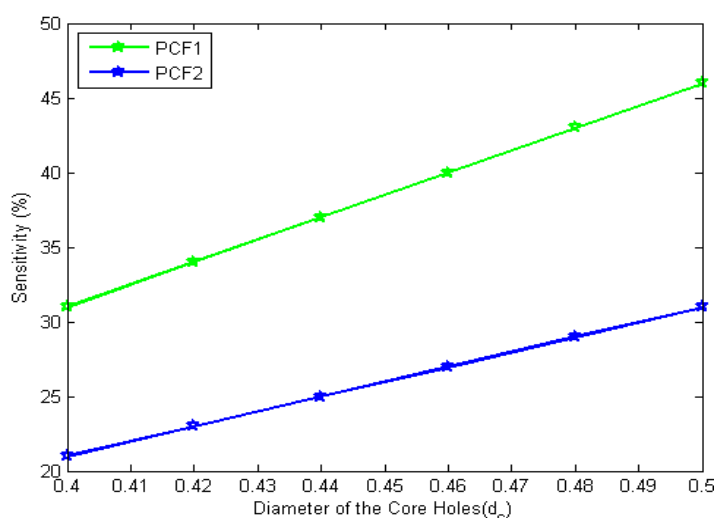


Figure 7 Variations of relative sensitivity as a function of supplementary core holes diameter ( $d_c$ ) for PCF<sub>1</sub> and PCF<sub>2</sub>

From the overall discussion, it can be found that the proposed PCF<sub>1</sub> shows better performance than PCF<sub>2</sub> in terms of relative sensitivity. In addition, both of the proposed PCFs show a great potentiality for liquid sensing applications. Table 2 demonstrates the comparative performance

analysis on the basis of simulated results between the proposed PCFs and prior PCFs for Ethanol sensing at the wavelength  $\lambda = 1.3 \mu\text{m}$ .

Table 2 Comparative performance analysis between the proposed PCFs and prior PCFs

PCFs	Ethanol (Refractive Index=1.353)		Structural Description
	Sensitivity (%)	Confinement Loss (dB/m)	
Ademgil (2014)	21.55	$5.65 \times 10^{-9}$	Cladding: 3 rings (Octagonal-Octagonal-Octagonal) Core: Microstructured with supplementary holes (Octagonal shape)
Asaduzzaman et al. (2015)	31.26	$8.75 \times 10^{-9}$	Cladding: 3 rings (Hexagonal-Octagonal-Octagonal) Core: Microstructured with supplementary holes (rectangular shape)
Proposed PCF <sub>1</sub>	39	$3.23 \times 10^{-7}$	Cladding: 3 rings (Hexagonal-Octagonal-Octagonal) Core: Microstructured with supplementary holes (Octagonal shape)
Proposed PCF <sub>2</sub>	33	$2.57 \times 10^{-9}$	Cladding: 3 rings (Hexagonal-Octagonal-Octagonal) Core: Microstructured with supplementary holes (Octagonal shape)

From the experimental point of view, it is important to discuss the fabrication process of the proposed PCFs. Micro-holes in the core must be filled with the sample (Ethanol) to be detected without damaging the integrity of fiber. Arrangement of the tiny holes in the core region and filling them with materials demonstrates the complexity of our proposed PCFs and it might be possible drawback of our proposed PCF structures. However, due to the progress of nanotechnology, the fabrication of our proposed PCFs is possible (Arif et al., 2016; Morshed et al., 2015b).

Several fabrication processes, such as selective-filling technique (Huang et al., 2004), high-pressure chemical vapor deposition (CVD) technique (Wolfbeis, 2008), allow the deposition of chemicals or any fluids into the cladding holes as well as the tiny core holes. Now, applying sol-gel technique (Bise & Trevor, 2005), any kind of complexity of fabrication can be removed. From the previously published papers (Xiao et al., 2005; Cordeiro et al., 2006b) it is clear that our proposed structures can be interfaced with these existing technologies.

## 6. CONCLUSION

From the numerical analysis, it is evidently clear that circular air holes in the first ring are responsible for higher sensitivity and square air holes in the first ring are responsible for the lower confinement loss. Therefore, both the proposed PCFs can overcome the critical trade-off between confinement loss and sensitivity. Although in this study, the relative sensitivity, confinement loss, and the effective index's features have been numerically investigated for

sensing Ethanol, it is expected that the proposed PCFs will be able to sense all types of liquid chemicals.

## 7. ACKNOWLEDGEMENT

The authors are grateful to those who participated in this research work.

## 8. REFERENCES

- Ademgil, H., 2014. Highly Sensitive Octagonal Photonic Crystal Fiber based Sensor. *Optik-International Journal for Light and Electron Optics*, Volume 125(20), pp. 6274–6278
- Arif, M.F.H., Ahmed, K., Asaduzzaman, S., Azad, M.A.K., 2016. Design and Optimization of Photonic Crystal Fiber for Liquid Sensing Applications. *Photonic Sensors*, Volume 6(3), pp. 279–288
- Asaduzzaman, S., Ahmed, K., Arif, M.F.H., Morshed, M., 2015. Application of Microarray-Core based Modified Photonic Crystal Fiber in Chemical Sensing. *In: Proceedings of the International Conference on Electrical and Electronic Engineering (ICEEE)*, Rajshahi, 04–06 November 2015, Bangladesh
- Balaji, T., El-Safty, S.A., Matsunaga, H., Hanaoka, T., Mizukami, F., 2006. Optical Sensors based on Nanostructured Cage Materials for the Detection of Toxic Metal Ions. *Angewandte Chemie*, Volume 118(43), pp. 7360–7366
- Birks, T.A., Knight, J.C., Russell, P.S.J., 1997. Endlessly Single-mode Photonic Crystal Fiber. *Optics Letters*, Volume 22(13), pp. 961–963
- Bise, R.T., Trevor, D.J., 2005. Sol-gel Derived Microstructured Fiber: Fabrication and Characterization. *In: Proceedings of the Optical Fiber Communications Conference (OFC)*, Anaheim, California, 6 March, USA
- Cárdenas-Sevilla, G.A., Finazzi, V., Villatoro, J., Pruneri, V., 2011. Photonic Crystal Fiber Sensor Array based on Modes Overlapping. *Optics Express*, Volume 19(8), pp. 7596–7602
- Carvalho, J.P., Lehmann, H., Bartelt, H., Magalhaes, F., Amezcua-Correa, R., Santos, J.L., Van Roosbroeck, J., Araújo, F.M., Ferreira, L.A., Knight, J.C., 2009. Remote System for Detection of Low-levels of Methane based on Photonic Crystal Fibres and Wavelength Modulation Spectroscopy. *Journal of Sensors*, Volume 2009, pp. 1–10
- Cordeiro, C., Dos Santos, E.M., Brito Cruz, C.H., de Matos, C.J., Ferreira, D.S., 2006a. Lateral Access to the Holes of Photonic Crystal Fibers—selective Filling and Sensing Applications. *Optics Express*, Volume 14(18), pp. 8403–8412
- Cordeiro, C., Franco, M.A., Chesini, G., Barretto, E., Lwin, R., Brito Cruz, C.H., Large, M.C., 2006b. Microstructured-core Optical Fibre for Evanescent Sensing Applications. *Optics Express*, Volume 14(26), pp. 13056–13066
- Hu, D.J.J., Lim, J.L., Park, M.K., Kao, L.T.H., Wang, Y., Wei, H.Y., Tong, W., 2012. Photonic Crystal Fiber-based Interferometric Biosensor for Streptavidin and Biotin Detection. *IEEE Journal of Selected Topics in Quantum Electronics*, Volume 18(4), pp. 1293–1297
- Huang, Y., Xu, Y., Yariv, A., 2004. Fabrication of Functional Microstructured Optical Fibers through a Selective-filling Technique. *Applied Physics Letters*, Volume 85(22), pp. 5182–5184
- James, D., Scott, S.M., Ali, Z., O'hare, W.T., 2005. Chemical Sensors for Electronic Nose Systems. *Microchimica Acta*, Volume 149(1-2), pp. 1–17
- Knight, J.C., Birks, T.A., Russell, P.S.J., Atkin, D.M., 1996. All-silica Single-mode Optical Fiber with Photonic Crystal Cladding. *Optics Letters*, Volume 21(19), pp. 1547–1549
- Kong, J., Franklin, N.R., Zhou, C., Chapline, M.G., Peng, S., Cho, K., Dai, H., 2000. Nanotube Molecular Wires as Chemical Sensors. *Science*, Volume 287(5453), pp. 622–625

- Lee, S., Park, J., Jeong, Y., Jung, H., Oh, K., 2009. Guided Wave Analysis of Hollow Optical Fiber for Mode-coupling Device Applications. *Journal of Lightwave Technology*, Volume 27(22), pp. 4919–4926
- McCague, C., Fabian, M., Karimi, M., Bravo, M., Jaroszewicz, L.R., Mergo, P., Sun, T., Grattan, K.T., 2014. Novel Sensor Design using Photonic Crystal Fibres for Monitoring the Onset of Corrosion in Reinforced Concrete Structures. *Journal of Lightwave Technology*, Volume 32(5), pp. 891–896
- Morshed, M., Arif, M.F.H., Asaduzzaman, S., Ahmed, K., 2015a. Design and Characterization of Photonic Crystal Fiber for Sensing Applications. *European Scientific Journal*, Volume 11(12), pp. 228–235
- Morshed, M., Hasan, M.I., Razzak, S.A., 2015b. Enhancement of the Sensitivity of Gas Sensor based on Microstructure Optical Fiber. *Photonic Sensors*, Volume 5(4), pp. 312–320
- Olyaei, S., Naraghi, A., Ahmadi, V., 2014. High Sensitivity Evanescent-field Gas Sensor based on Modified Photonic Crystal Fiber for Gas Condensate and Air Pollution Monitoring. *Optik-International Journal for Light and Electron Optics*, Volume 125(1), pp. 596–600
- Pinto, A.M., Lopez-Amo, M., 2012. Photonic Crystal Fibers for Sensing Applications. *Journal of Sensors*, Volume 2012, pp. 1–21
- Sellmeier, W., 1871. Zurerklärung der Abnormenfarbenfolgeim Spectrum Einigersubstanzen. *Annalen der Physik und Chemie*, Volume 219(6), pp. 272–282
- Stewart, G., Norris, J., Clark, D.F., Culshaw, B., 1991. Evanescent-wave Chemical Sensors—A Theoretical Evaluation. *International Journal of Optoelectronics*, Volume 6(3), pp. 227–238
- Whitenett, G., Stewart, G., Atherton, K., Culshaw, B., Johnstone, W., 2003. Optical Fibre Instrumentation for Environmental Monitoring Applications. *Journal of Optics A: Pure and Applied Optics*, Volume 5(5), pp. S140–S145
- Wolfbeis, O.S., 2008. Fiber-optic Chemical Sensors and Biosensors. *Analytical Chemistry*, Volume 80(12), pp. 4269–4283
- Xiao, L., Jin, W., Demokan, M., Ho, H., Hoo, Y., Zhao, C., 2005. Fabrication of Selective Injection Microstructured Optical Fibers with a Conventional Fusion Splicer. *Optics Express*, Volume 13(22), pp. 9014–9022